

## The Immune Response to Chronic *Pseudomonas aeruginosa* Wound Infection in Immunocompetent Mice

Johanna M. Sweere,<sup>1,2</sup> Heather Ishak,<sup>3</sup> Vivekananda Sunkari,<sup>1</sup> Michelle S. Bach,<sup>1</sup> Robert Manasherob,<sup>1</sup> Koshika Yadava,<sup>1,4</sup> Shannon M. Ruppert,<sup>1</sup> Chandan K. Sen,<sup>5</sup> Swathi Balaji,<sup>6</sup> Sundeeep G. Keswani,<sup>6</sup> Patrick R. Secor,<sup>7</sup> and Paul L. Bollyky<sup>1,\*</sup>

<sup>1</sup>Division of Infectious Diseases and Geographic Medicine, Department of Medicine, Stanford University, Stanford, California.

<sup>2</sup>Stanford Immunology, Stanford University, Stanford, California.

<sup>3</sup>Department of Neurology, Palo Alto Veterans Institute of Research, Palo Alto, California.

<sup>4</sup>Medical Sciences Division, University of Oxford, Oxford, United Kingdom.

<sup>5</sup>Department of Surgery, Indiana University School of Medicine, Indiana University, Bloomington, Indiana.

<sup>6</sup>Division of Pediatric Surgery, Department of Surgery, Baylor College of Medicine, Houston, Texas.

<sup>7</sup>Division of Biological Sciences, University of Montana, Missoula, Montana.

**Objective:** Our goal was to develop a chronic wound model in mice that avoids implantation of foreign material or impaired immunity and to use this to characterize the local and systemic immune response associated with *Pseudomonas aeruginosa* infection.

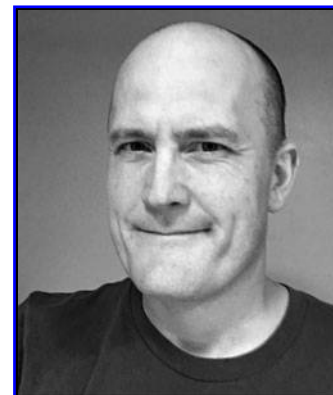
**Approach:** We generated bilateral full-thickness dermal wounds in healthy 10–12-week-old C57Bl6 mice. We waited 24 h to inoculate the developing wound eschar at these sites. We performed careful titration experiments with luminescent strains of *P. aeruginosa* to identify bacterial inoculation concentrations that consistently established stable infections in these animals. We performed flow cytometry-based immunophenotyping of immune cell infiltrates at the wound site, spleen, and draining lymph nodes over time. Finally, we compared inflammatory responses seen in wound inoculation with planktonic bacteria, preformed biofilm, and heat-killed (HK) *P. aeruginosa*.

**Results:** Using this delayed inoculation model and  $7.5 \pm 2.5 \times 10^2$  CFU/mL of PAO1 we consistently established stable infections that lasted at 10 days in duration. During early infection, we detected a strong upregulation of inflammatory cytokines and neutrophil infiltration at the wound site, while natural killer (NK) cells and dendritic cells (DCs) were reduced. At the systemic level, only plasmacytoid DCs were increased early in infection. During later stages, there was systemic upregulation of B cells, T cells, and macrophages, whereas NK cells and interferon killer DCs were reduced. Infections with *P. aeruginosa* biofilms were not more virulent than infections with planktonic *P. aeruginosa*, whereas treatment with HK *P. aeruginosa* only induces a short-term inflammatory state.

**Innovation:** We describe a versatile wound model of chronic *P. aeruginosa* infection that lasts 10 days without causing sepsis or other excessive morbidity.

**Conclusion:** This model may facilitate the study of chronic wound infections in immunocompetent mice. Our findings also highlight the induction of early innate immune cell populations during *P. aeruginosa* infection.

**Keywords:** *Pseudomonas*, wound model, immune profiling, chronic infection



Paul L. Bollyky, MD, PhD

Submitted for publication June 6, 2019. Accepted in revised form June 27, 2019.

\*Correspondence: Division of Infectious Diseases and Geographic Medicine, Department of Medicine, Stanford University, Beckman B241, 279 Campus Drive, Stanford, CA 94305 (e-mail: pbollyky@stanford.edu).

## INTRODUCTION

*PSEUDOMONAS AERUGINOSA* is a bacterial pathogen associated with morbidity, mortality, and poor quality of life in a variety of human infections including burns, leg ulcers, and lung infections.<sup>1-3</sup> Its clinical importance and rising incidence of antibiotic resistance has led to increased interest in understanding how the immune system can clear—or fail to clear—*P. aeruginosa* from sites of injury, and how the immune response changes from the acute stages of infection to the chronic stages of infection.<sup>4-8</sup>

The presence of an injury naturally activates local immune populations, primarily by attracting neutrophils to the site of injury to protect from infection. If no infection occurs and the healthy injury starts to heal, an influx of macrophages engulf the now apoptotic neutrophils and signal for the resolution of inflammation. An alteration in this process, such as is present during infection with *P. aeruginosa*, can cause a persistent state of inflammation and aberrant healing.<sup>4</sup> Cytokines are important mediators of these processes by keeping a precarious balance between resisting infection and minimizing tissue damage. For example, tumor necrosis factor (TNF) secretion is a healthy part of the inflammatory stage of injury response.<sup>5</sup> TNF can be upregulated by activation of the NF $\kappa$ B pathway in response to bacterial components and play a critical role for the clearance of *P. aeruginosa*.<sup>6</sup> However, persistent presence of inflammatory components lead to excessive production of TNF and IL-1 $\beta$ , which can lead to tissue damage, persistence of infection, morbidity, and mortality.<sup>7</sup> A similar dual role in providing protection only when secreted in moderation has been seen for IL-17.<sup>8</sup> Therefore, a better understanding of the regulation of immunological processes happening at the infected injury site, especially the innate immune response, may improve therapeutic strategies against *P. aeruginosa*.

## CLINICAL PROBLEM ADDRESSED

Improved mouse models are needed to aid in the investigation of chronic wound infections. Unfortunately, healthy adult mice often either rapidly resolve or succumb to infections in many experimental systems. Therefore, most models either utilize mice with impaired immunity or introduce foreign materials that serve as a nidus of infection.<sup>9-12</sup> This is potentially problematic because diabetic, obese, or aged mice may not entirely exhibit normal immunity. Foreign materials, such as agar beads, silicone implants, or alginate gels, may likewise alter local inflammatory processes.

Consequently, there is a dearth of knowledge about the pathophysiology of chronic wound infections in immunologically normal hosts. Moreover, much of the available information on the immunology of wound infections takes the form of histological studies and semiquantitative scoring. This complicates immunophenotyping and quantification of wound immune cell types leading to a paucity of information on the nature of local and systemic immunity associated with chronic wound infections.

Considering these issues, we set out to develop a chronic infection model that allowed for assessments of local and systemic immune responses against *P. aeruginosa*.

## MATERIALS AND METHODS

### Mice

Mice were bred and maintained under specific pathogen-free conditions, with free access to food and water, in the vivarium at Stanford University. Mice that underwent surgery received additional Supplical Pet Gel (Henry Schein Animal Health, Cat. No. 029908) and intraperitoneal injections of sterile saline (Hospira, Cat. No. 0409-4888-10). All mice used for *in vivo* infection experiments were littermates. Conventional C57BL/6J mice were purchased from The Jackson Laboratory (Bar Harbor, ME). All experiments and animal use procedures were approved by the Institutional Animal Care & Use Committee at the School of Medicine at Stanford University.

### Chemicals, antibiotics and reagents

The following chemicals, antibiotics and reagents were used: lipopolysaccharide from *Escherichia coli* O111:B4 (Sigma, Cat. No. L4391); alginic acid (Sigma, Cat. No. A0682); bovine serum albumin (Fisher Bioreagents, Cat. No. BP1600); heat-inactivated fetal bovine serum (RMBIO, Cat. No. FBS-BHT-5XM); RPMI (HyClone, Cat. No. SH30027.01); penicillin and streptomycin solution (Corning, Cat. No. MT30002CI), sodium pyruvate (HyClone, Cat. No. SH3023901); tryptone (Fluka Analytical, Cat. No. T7293); sodium chloride (Acros Organics, Cat. No. 7647-14-5); yeast extract (Boston BioProducts, Cat. No. P-950); agar (Fisher BioReagents, Cat. No. BP9744); gentamicin (Amresco, Cat. No. E737); carbenicillin (Gold Biotechnology, Cat. No. C-103-25) and kanamycin (Fisher BioReagents, Cat. No. BP906).

### Bacterial strains and culture conditions

*P. aeruginosa* strain PAO1 was used for all experiments unless stated otherwise and was cultured as previously described<sup>13</sup>. In general, frozen

glycerol stocks were streaked on Luria-Bertani (LB) agar containing selective antibiotics (PAO1 and clinical strains: none; luminescent strains: 100  $\mu\text{g}/\text{mL}$  carbenicillin and 12.5  $\mu\text{g}/\text{mL}$  kanamycin) and grown overnight at 37°C. An isolated colony was picked and grown overnight at 37°C in LB medium, pH 7.4 (for luminescent strains, broth contained 100  $\mu\text{g}/\text{mL}$  carbenicillin) under shaking, aerobic conditions. For preparation of heat-killed bacteria frozen glycerol stocks were streaked on LB agar. Individual colonies were grown in 5 mL of LB broth the next day for 2 h to approximately  $2 \times 10^8$  CFU/mL. The bacterial cultures were centrifuged at  $6,000 \times g$  for 5 min, and the pellet was washed in 1 mL of PBS three times. Finally, the pellet was resuspended in 1 mL of PBS and heated for 30 min at 90°C under shaking conditions. The preparation was checked for sterility by plating as previously described.<sup>14</sup> Bioluminescent bacteria were generated as previously reported.<sup>15</sup>

#### ***In vivo* murine full-thickness wound infection model**

Ten-to-twelve-week old male mice were anesthetized, shaved and received two dorsal excisional wounds, as previously described.<sup>16</sup> The wound area was washed with saline and covered with Tegaderm (3M, Cat. No. 1642W). Luminescent bacteria were grown as described above and diluted to the standard dose of  $7.5 \pm 2.5 \times 10^2$  CFU/mL or  $1 \times 10^7$  CFU/mL in PBS. Mice were inoculated with 40  $\mu\text{L}$  per wound 24 h post-wounding, and control mice were inoculated with sterile PBS. In some experiments, mice received a dose of  $1 \times 10^7$  CFU/mL heat-killed bacteria, prepared as described above. Mice were weighed and imaged for luminescent signal on the IVIS Spectrum (Perkin Elmer), the Ami HTX (Spectral Instruments Imaging) or the Lago-X (Spectral Instruments Imaging) at the Stanford Center for Innovation in *In Vivo* Imaging daily before takedown. Uninfected mice were photographed for luminescent background correction. Images were subsequently analyzed using Living Image Software (Perkin Elmer), AMIView Software (Spectral Instruments Imaging) or Aura software (Spectral Instruments Imaging). Upon takedown, wound beds were excised and processed to enumerate bacterial burden. Wounds were considered infected if luminescent signal in the wound was above background luminescence, and bacteria were detected in the wound effluent. Wounds were harvested, bifurcated, fixed in 10% neutral buffered formalin, and embedded in paraffin as previously described.<sup>17</sup>

#### **Mouse wound, spleen and lymph node harvesting and immunophenotyping**

Mouse wounds were excised with scissors, cut into pieces and collected in RPMI containing 0.025 mg/mL Liberase TM Research Grade (Roche, Cat. No. 5401127001), 50  $\mu\text{M}$  2-mercaptoethanol (Sigma, Cat. No. M3148) and 20 mM HEPES (Teknova, Cat. No. 101446-740). Tissue was digested at 37°C for 2 h, homogenized through a sterile 1-mL syringe (BD Biosciences, Cat. No. 309659) and passed through a 70  $\mu\text{m}$  cell strainer (Fisherbrand, Cat. No. 22363548). Cells were washed twice with PBS at  $300 \times g$  for 5 min and processed according to the flow cytometry protocol.

Murine spleen and lymph node were harvested and treated as previously described.<sup>18</sup> In brief, this was done in RPMI-10, dissociated in a 70- $\mu\text{m}$  cell strainer using the plunger of a 1-mL syringe, and washed with RPMI-10 at  $300 \times g$  for 5 min. Splenocytes were treated with ACK lysis buffer containing 150 mM ammonium chloride (Fisher Chemical, Cat. No. A661), 10 mM potassium bicarbonate (Sigma, Cat. No. 237205) and 0.1 mM NaEDTA (PanReac AppliChem, Cat. No. A1104) for 5 min at room temperature and washed with RPMI-10 at  $300 \times g$  for 5 min. Cells were counted and used for assays as described.<sup>19</sup> For immunophenotyping, cells were lifted with cold PBS and processed according to our previously published flow cytometry protocol.<sup>20</sup> All immune cells from spleens, lymph nodes and wounds were stained with Zombie Aqua Viability Dye, B220, I-A/I-E, CD11c, CD11b<sup>+</sup>, F4/80, CD49b, Gr-1, CD3 and CD8 according to the flow cytometry protocol. Cells were divided into different leukocyte populations based on various cell surface markers: CD4<sup>+</sup> T cells (CD3<sup>+</sup>CD8<sup>-</sup>CD49b<sup>-</sup>); CD8<sup>+</sup> T cells (CD3<sup>+</sup>CD8<sup>+</sup>CD49b<sup>-</sup>); B cells (B220<sup>+</sup>I-A/I-E<sup>+</sup>); IKDCs (B220<sup>+</sup>CD49b<sup>+</sup>CD11c<sup>+</sup>), pDCs (B220<sup>+</sup>CD49b<sup>-</sup>CD11c<sup>+</sup>I-A/I-E<sup>+</sup>), cDCs (B220<sup>-</sup>CD11c<sup>+</sup>I-A/I-E<sup>+</sup>), NK cells (CD49b<sup>+</sup>CD3<sup>-</sup>), macrophages (CD11b<sup>+</sup>F4/80<sup>+</sup>), monocytes (CD11b<sup>+</sup>F4/80<sup>+</sup>Gr-1<sup>+</sup>) and neutrophils/eosinophils (Gr-1<sup>+</sup>CD11b<sup>+</sup>) according to our previously reported gating schemes.<sup>15</sup> Cells were processed and stained and flow cytometry was performed as previously described.<sup>18</sup> Analysis for this project was done on LSR II (BD Biosciences) instruments in the Stanford Shared FACS Facility.

#### **Statistical analysis**

Where  $n$  is not stated, graphs show a representative experiment of  $n \geq 2$  assays, with  $n \geq 3$  technical or biological replicates. The number of mice needed for the *in vivo* experiment was determined using power calculations. All statistical analyses, linear and nonlinear regression analyses

were performed using GraphPad Prism (GraphPad Software, Inc. La Jolla, CA). All unpaired Student's *t*-tests, Mann-Whitney tests, and Fisher's exact test were two-tailed. Depicted are means with SEM of the replicates unless otherwise stated. Statistical significance was considered  $p < 0.05$ . Non-significance was indicated by the letters n.s.

## RESULTS

### Development of a chronic wound infection model of *P. aeruginosa* using luminescent bacteria

The first objective of this study was to develop a mouse model of chronic infection that met the following requirements: (1) the infection is physiologically relevant; (2) the model requires no manipulation through use of foreign materials or immunosuppressants; (3) the model requires no use of immunosuppressed mice; (4) the infection does not lead to excessive morbidity or mortality; (5) the model could use planktonic *P. aeruginosa*, and (6) the infection can be tracked visually. Taking these considerations in mind, the decision was made to establish wounds in C57BL/6 mice, a strain that is widely used in immunology research, and to inoculate these with *P. aeruginosa*, one of the most common Gram-negative pathogens found in wound patients.<sup>21</sup> C57BL/6J mice are immunologically competent yet susceptible to *P. aeruginosa* infection.<sup>22</sup>

To generate this model, the dorsal skin of male C57BL/6J mice 10–12 weeks of age was shaved, depilated, and disinfected. Mice were treated with slow-release buprenorphine before receiving bilateral dorsal full-thickness, excisional wounds. The two wounds were treated as replicates, as previous studies have demonstrated that there is limited correlation between wounds within the same animals and bilateral wounds are therefore a good method to increase statistical power without increasing the number of animals.<sup>23</sup> Wounds were generated by excising a 6-mm-diameter circular wound area, outlined by a punch biopsy, using scissors.<sup>24</sup> The wounds were washed with saline and covered with Tegaderm for 24 h before inoculation with *P. aeruginosa* wound isolate strain PAO1 through injection underneath the Tegaderm. The 24-h delay before inoculation allowed for the formation of a nascent scab, which we hypothesized *P. aeruginosa* could colonize, to minimize the risk of sepsis. As Tegaderm is transparent, its usage allowed for daily inspection of the wound and protection from other contaminating bacteria. Notably, this model also does not require

foreign materials (other than Tegaderm) or immunosuppressants.

To facilitate the quantification of bacterial burden within infected wounds, we transformed PAO1 with a plasmid encoding the luxABCDE reporter system to generate luminescent bacteria (strain PAO1:lux). We inoculated mouse wounds with this strain and assessed bacterial burden over time by quantifying luminescence (Fig. 1A). While infections persist reliably out to 10 days in this model, we find that after 7 days, the PAO1:lux strain begin to lose production of luminescence despite obvious ongoing infection. For this reason, the schematic here is shown, in this iteration, as a 7-day protocol but elsewhere in the article 10-day experiments are reported that did not involve tracking luminescence.

Inoculation resulted in a clearly detectable luminescent signal around the edges of the wound, indicating that *P. aeruginosa* embeds itself in the skin layers surrounding the wound (Fig. 1B). Infection with luminescent PAO1 peaked at around day 3 postinoculation but reliably persisted at least 7 days postinoculation (Fig. 1C, D). This model was carried out as long as 2 weeks, but heterogeneity between mice limited the utility of later time points (data not shown). Isolation of the bacteria from the wound demonstrated that CFU/wound correlated with detected luminescence (Fig. 1E). Mice rapidly started losing weight immediately after infection, with some animals losing up to 20% of their weight 2 days postinoculation (Fig. 1F). However, intraperitoneal saline injections and supplemental food in the form of suppicall liquid gel restored the health of these mice to acceptable levels (Fig. 1F).

We next calculated the inoculation dose at which the majority (>50%) of wounds would become sustainably infected with PAO1. We assessed the presence or absence of bacterial infection 3 days postinoculation by quantifying luminescence. This time point was chosen because it was observed in preliminary studies that the infection rate was stable after that time. Careful titration of inoculation doses with luminescent PAO1 revealed that PAO1 had an ID<sub>50</sub> value of  $\sim 7.7 \times 10^2$  CFU/mL in this wound infection model (Fig. 1G). Doses higher than  $10^4$  CFU/mL generally resulted in 100% infection rate (Fig. 1G).

### Early wound infection is marked by influx of neutrophils and reduction of natural killer cells and dendritic cells

Using this infection model, we assessed the local immunological response to *P. aeruginosa* wound infection. We first focused on the early stages of infection. We infected our mice with either live bacteria as

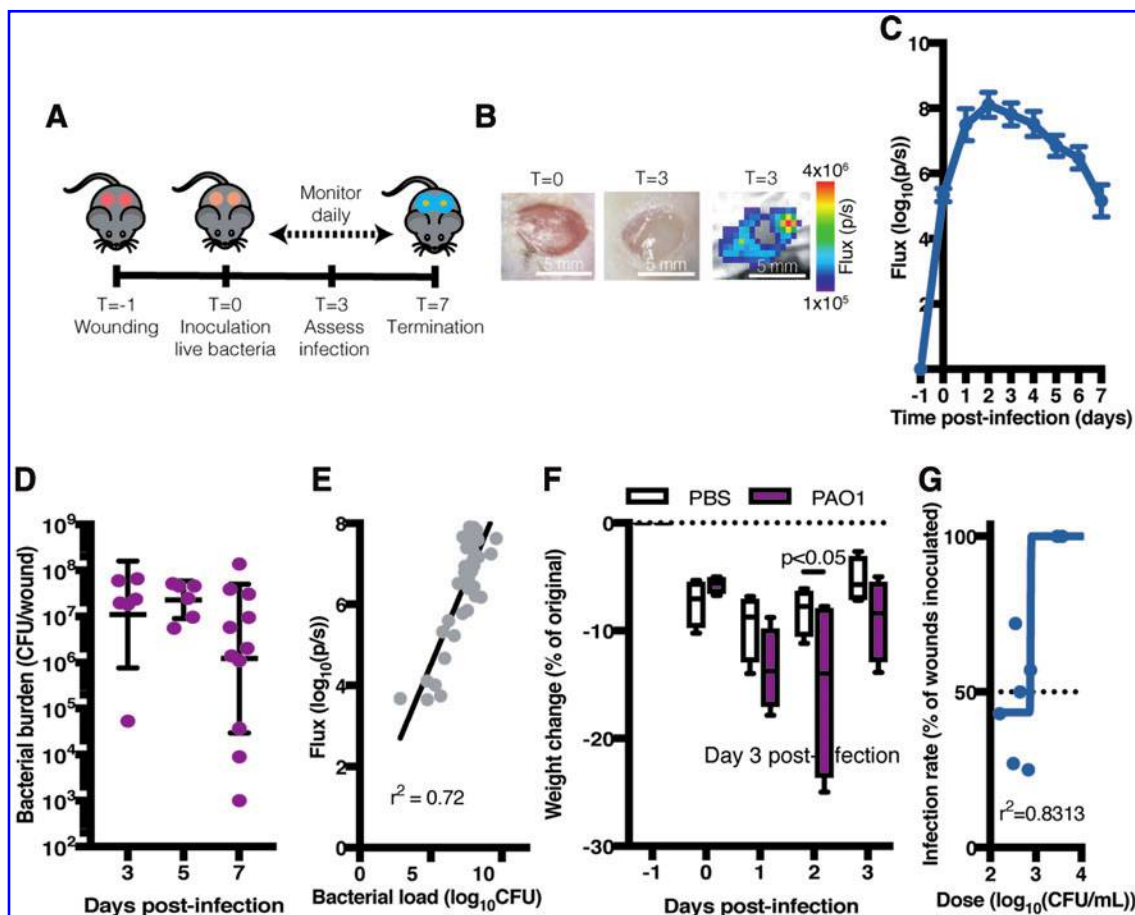


**Figure 1.** Development of a novel *P. aeruginosa* wound infection model. **(A)** Schematic of the general full-thickness wound infection model with luminescent bacteria. While infections persist reliably out to 10 days in this model, we find that after 7 days the PAO1:lux strain begin to lose production of luminescence despite obvious ongoing infection. For this reason this schematic here is shown as a 7-day protocol. **(B)** Representative images of murine wounds pre- (*left*) and postinfection (*middle*) showing luminescent bacterial signal (*right*). **(C)** Luminescent signal reflecting wound bacterial burden.  $N=6$  wounds. Inoculation:  $10^5$  CFU/mL PAO1. **(D)** Wound bacterial burden in CFU/wound over time in mice infected with  $10^5$  CFU/mL PAO1. Depicted are geometric mean and geometric SD. **(E)** Linear regression analysis of *in vivo* luminescent signal and bacterial CFU of PAO1:lux-infected wounds, collected 4–7 days postinoculation with  $10^5$  CFU/mL to allow for range of bacterial burdens. **(F)** Weight change (relative to weight before surgery on  $T=-1$ ) in mice infected according to the schematic in **(A)**.  $n=4$  mice/group. Depicted are boxplots for 5–95 percentile. Statistics are two-way ANOVA corrected with Sidak multiple comparison. **(G)** Nonlinear regression analysis of wound infection rate plots used to calculate the  $IC_{50}$  for PAO1 3 days postinoculation. All graphs are representative of  $n \geq 3$  experiments. Color images are available online.

described above or phosphate buffered saline (PBS) as a control. After 3 days, we analyzed the immune cell populations present in the wound beds using flow cytometry (Fig. 2A).

We observed a substantial (approximately four-fold) increase in the amount of neutrophils present (Fig. 2B), consistent with their role in the early inflammatory response during wound healing and infection.<sup>25</sup> Interestingly, there was a local decrease in the amount of skin natural killer (NK) cells and dendritic cells (DCs) (Fig. 2C, D). Further subdivision of the skin DCs into distinct subsets revealed that the most notable decreases were seen in  $CD11b^+$  DCs and Gr1-low monocyte-derived DCs (MoDCs) (Fig. 2E), which are MoDCs in a state of inflammatory activation.<sup>26</sup> There was no significant difference in the number of macro-

phages present in the skin (data not shown). These data indicate that the local immune response to *P. aeruginosa* early in infection is marked by differences in neutrophils, NK cells, and DCs.

### Early wound infection induces lymph node plasmacytoid DCs

We hypothesized that the local decrease in NK cells and DCs in response to *P. aeruginosa* wound infection was due to migration of these immune cell populations to the spleen or draining lymph nodes (LNs), where they could direct systemic immune responses. Therefore, we analyzed the immune cell populations present in the spleen and draining peripheral LN 3 days postwound infection using flow cytometry (Fig. 3A). First, we looked at adaptive immune responses and saw a nonsignificant

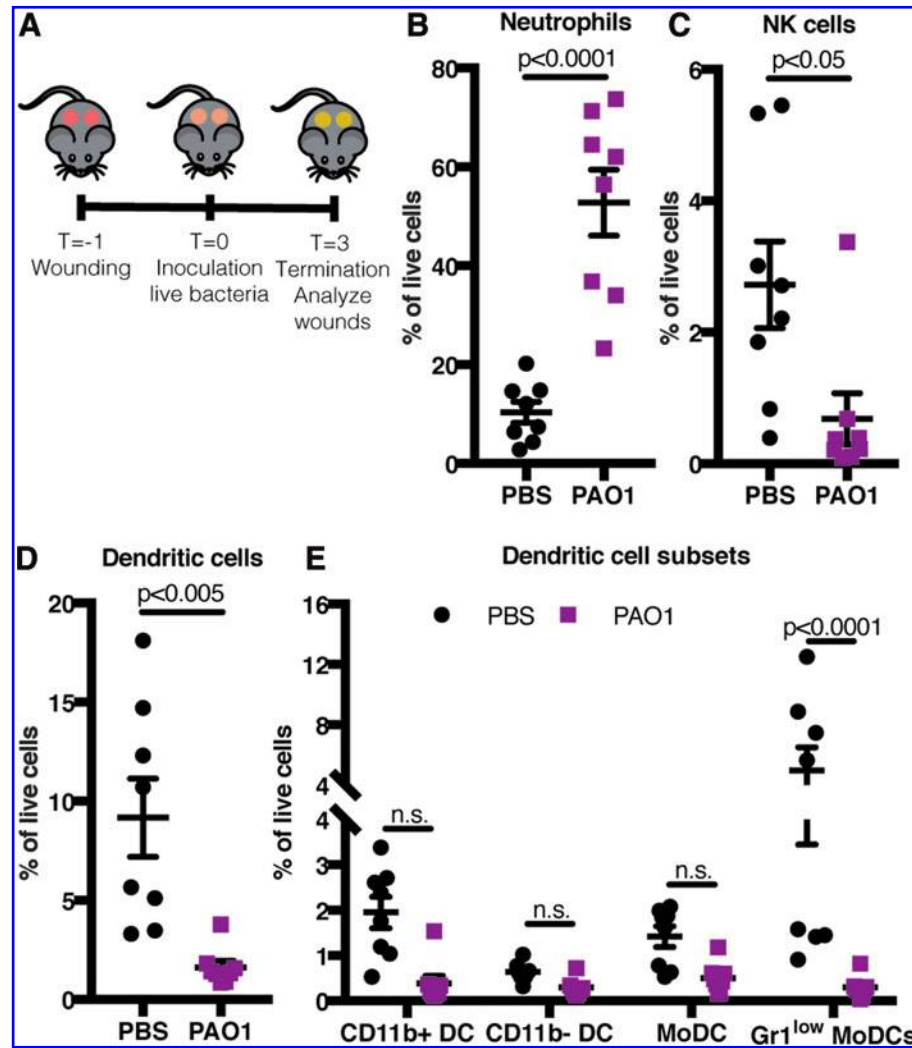


**Figure 2.** Acute (day 3 postwounding) wound infection with *P. aeruginosa* is marked by changes in wound neutrophil, NK cell, and DC populations. **(A)** Schematic for wound infiltrate analysis through enzymatic digestion after acute wound infection. Shown are wound infiltrates for **(B)** neutrophils; **(C)** NK cells, and **(D)** DCs in the wounds of mice infected according to the schematic in **(A)**. Statistics are two-tailed Student's *t*-test. **(E)** Wound DC infiltrates from **(D)** divided into distinct DC subsets. MoDC= monocyte-derived DCs. Statistics are two-way ANOVA corrected with Sidak multiple comparison. **(B, C)** depict mean with SEM and are representative of  $n \geq 2$  experiments. DC, dendritic cell; NK, natural killer. Color images are available online.

trend toward increased B cell spleen and LN populations (Fig. 3B).

We observed a significant reduction in splenic T cells (Fig. 3C). There was no significant difference in the amount of preapoptotic T cells (Fig. 3D), identified as B220<sup>+</sup>CD3<sup>+</sup>,<sup>27</sup> making cell death an unlikely cause for the observed decline. We also detected nonsignificant increases in splenic neutrophils and macrophages (Fig. 3E, F). Surprisingly, we also observed a nonsignificant decrease in splenic NK cells (Fig. 3G), suggesting that the decrease in skin NK cells is not due to migration to secondary lymphoid organs. Finally, we looked at DC subsets known to be present in spleen and LNs, including interferon killer DCs (IKDCs), plasmacytoid DCs (pDCs), and conventional (classical)

DCs (cDCs). There was a significant increase in LN pDCs and a less marked increase in splenic pDCs (Fig. 3H). Infection induced no differences in IKDCs (Fig. 3I) or cDCs (Fig. 3J).

Altogether, these data indicate that during the early stages of wound infection with *P. aeruginosa*, the systemic immune system is not prominently affected.

#### Late-stage wound infection predominantly impacts systemic innate immune responses

We next examined spleen and LN immune cell populations at later stages of infection. To that end, we used the same mouse model of infection as in Fig. 1A, but added a silicone ring around the mouse wound at the time of wounding to prevent me-

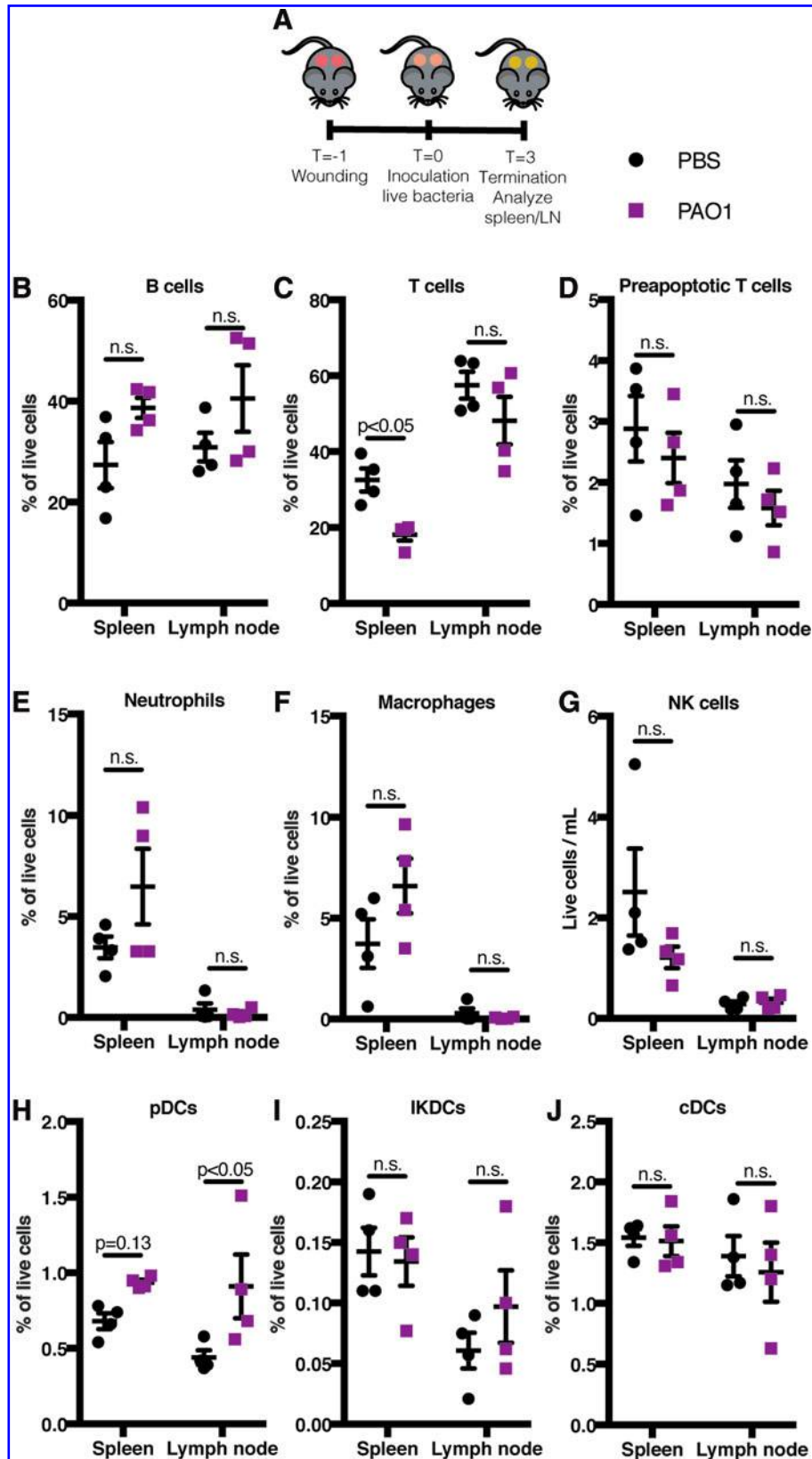


**Figure 3.** Acute wound infection with *P. aeruginosa* is marked by few changes in spleen and peripheral LN immune populations. **(A)** Schematic for spleen and peripheral LN immune population analysis after acute wound infection. Shown are the spleen and LN populations for **(B)** B cells, **(C)** T cells, **(D)** preapoptotic T cells, **(E)** neutrophils, **(F)** macrophages, **(G)** NK cells, **(H)** pDCs, **(I)** IKDCs, and **(J)** cDCs in mice infected according to the schematic in **(A)**. Statistics are two-tailed Student's *t*-test. **(B–J)** depict mean with SEM and are representative of  $n \geq 2$  experiments. cDCs, conventional (classical) DCs; IKDCs, interferon killer DCs; LN, lymph node; pDCs, plasmacytoid DCs. Color images are available online.

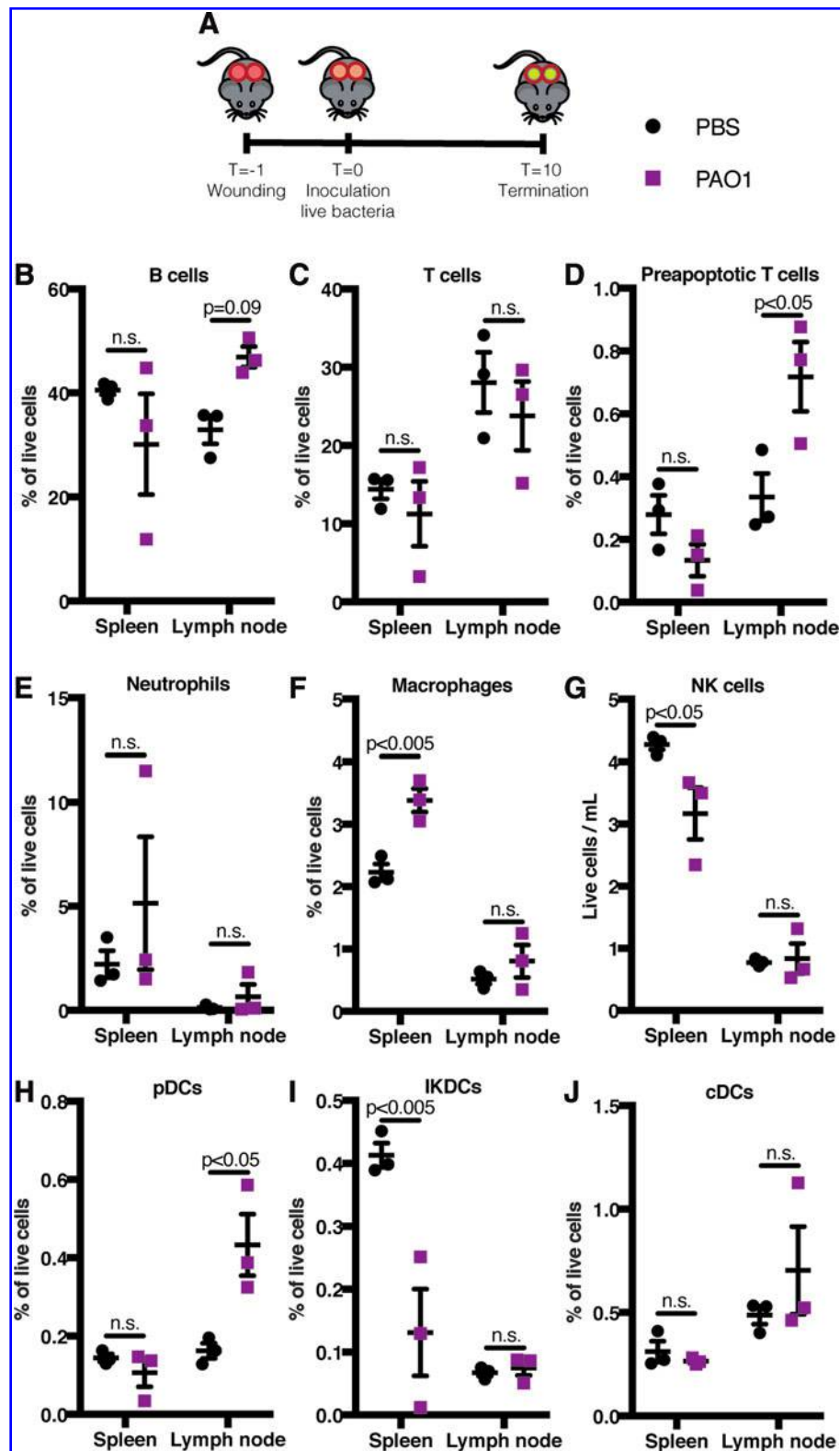


**Figure 4.** Chronic (day 10 postwounding) wound infection with *P. aeruginosa* is marked by changes in spleen and peripheral LN innate, but not adaptive immune cell populations. **(A)** Schematic for spleen and peripheral LN immune population analysis after chronic wound infection. Shown are the spleen and LN populations for **(B)** B cells, **(C)** T cells, **(D)** preapoptotic T cells, **(E)** neutrophils, **(F)** macrophages, **(G)** NK cells, **(H)** pDCs, **(I)** IKDCs, and **(J)** cDCs in mice infected according to the schematic in **(A)**. Statistics are two-tailed Student's *t*-test. **(B–J)** depict mean with SEM and are representative of  $n \geq 2$  experiments. Color images are available online.

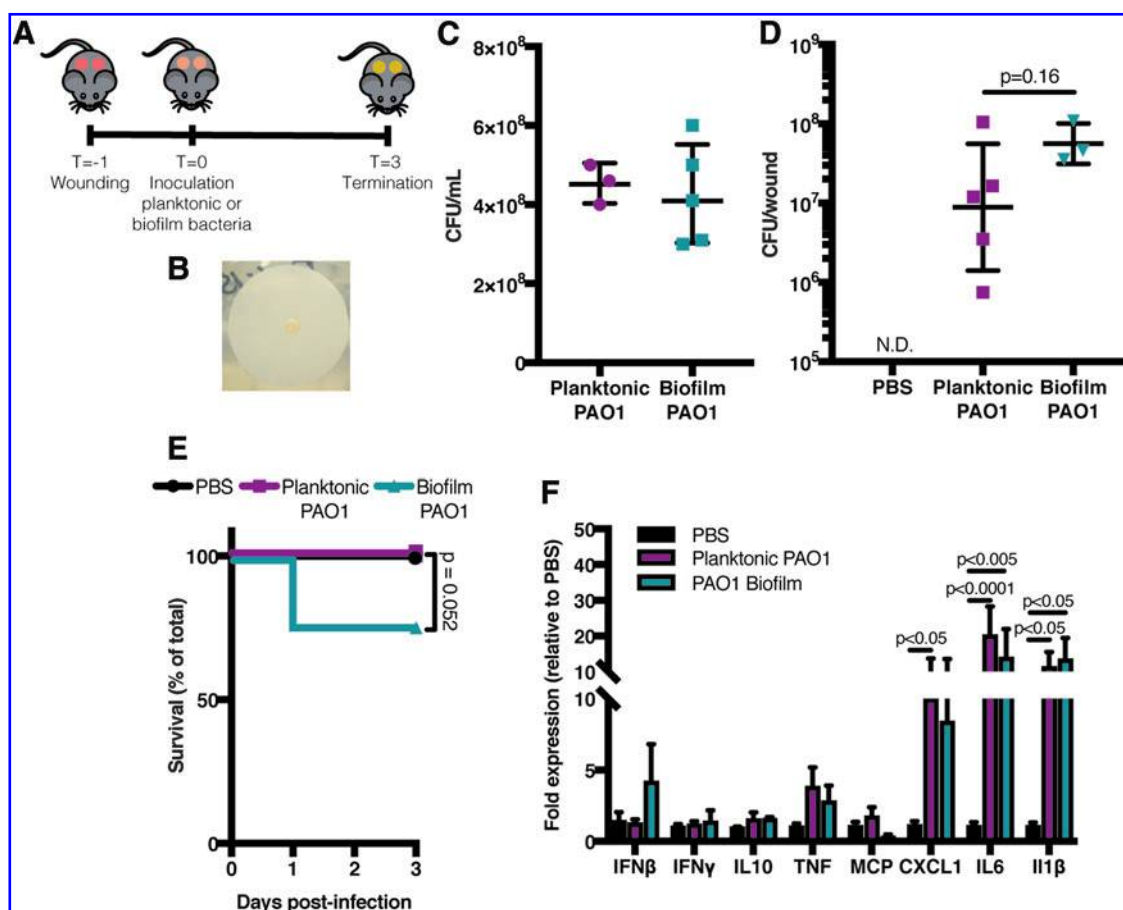


**Figure 5.** Biofilm infections with *P. aeruginosa* are not more lethal than planktonic infections in this model. **(A)** Schematic of the general full-thickness wound infection model with biofilm bacteria. **(B)** Image of *P. aeruginosa* biofilm culture. **(C)** Inoculation doses of planktonic and biofilm PAO1 strains. **(D)** Wound bacterial burden in CFU/wound on T=3 in mice infected according to the schematic in **(A)**. Statistics are two-tailed Student's *t*-test. Depicted in **(C, D)** are geometric mean and geometric SD. **(E)** Survival in mice after wound infection with planktonic or biofilm PAO1 ( $n=8-10$ /group; log-rank Mantel-Cox test). **(F)** mRNA fold expression (relative to PBS) of several inflammatory cytokines at the wound site after acute infection with planktonic or biofilm PAO1 using  $\beta$ -actin as a household gene.  $n=3-5$  wounds/group. Statistics are two-way ANOVA with Dunnett multiple comparison to PBS. Plot depicts mean with SD and is representative of  $n \geq 2$  experiments. PBS, phosphate buffered saline. Color images are available online.

chanotransduction and keep the wound open for longer periods of time.<sup>24</sup> Using this adjusted model, wounds stayed open and infected up to 10 days postinoculation (Fig. 4A).

There were no significant differences in B or T cell populations (Fig. 4B, C). However, at this later time point during infection, there was a significant increase in the amount of preapoptotic T cells (Fig. 4D), suggesting that T cells are activated during *P. aeruginosa* infection but prematurely dying.

Analysis of the systemic innate immune populations revealed no differences in neutrophil populations between infected and control mice (Fig. 4E), but a significant increase in splenic macrophages (Fig. 4F). These findings are consistent with the resolution of inflammation, which is typically mediated by macrophages.<sup>25</sup> Interestingly, splenic NK cells were significantly reduced in

infected mice during late infection (Fig. 4G). Next, analysis of DC subsets revealed a significant increase in LN pDCs (Fig. 4H) and a significant decrease in splenic IKDCs (Fig. 4I). Again, there were no differences in cDCs (Fig. 4J).

Combined with the findings in Figs. 2 and 3, these data suggest that changes in innate immune populations occur early and are sustained during the course of *P. aeruginosa* infection, but that the adaptive immune response is not markedly involved.

### Infection with preformed biofilm is more lethal than infection with planktonic *P. aeruginosa*

*P. aeruginosa* is notorious for its ability to form biofilm and protect itself against immune clearance by covering its colonies in a protective layer of slime.<sup>27</sup> Therefore, mice were infected

with *P. aeruginosa* in a preformed biofilm and immune responses at the wound site were monitored (Fig. 5A). *P. aeruginosa* was grown as a biofilm on a membrane for 48 h. The preformed biofilm, which contained  $\sim 5 \times 10^8$  CFU/mL, was then transferred to the wounds (Fig. 5B, C). For comparison, a treatment group was inoculated with an equivalent dose of about  $5 \times 10^8$  CFU/mL planktonic bacteria (Fig. 5C).

Analysis of bacterial burden 3 days postinoculation demonstrated no significant difference between the planktonic or biofilm *P. aeruginosa* treatment groups, but the range in bacterial burden between individuals was markedly less in the biofilm group (Fig. 5D). These findings perhaps reflect reduced bacterial migration from the wound site, suppressed immune clearance, or more efficient wound colonization in the biofilm group. There was no difference in survival between mice given planktonic or biofilm bacteria in this model (Fig. 5E).

Next, cytokine production at the site of wound infection between the different treatment groups was examined. Analysis of wound cytokine mRNA levels revealed that wound infection by either planktonic or biofilm infection with *P. aeruginosa* upregulated expression of TNF, CXCL1, IL-6, and IL-1 $\beta$  relative to wounds treated with PBS (Fig. 5F). TNF production was not as strongly upregulated as the other cytokines, probably because of the fact that TNF secretion in uninfected wounds is already high due to its pivotal role in wound healing. There were no significant differences in cytokine mRNA production between planktonic bacteria and biofilm-infected wounds, but there was a notable, yet nonsignificant, upregulation of interferon beta (IFN $\beta$ ) and a downregulation of MCP-1 in biofilm-infected wounds (Fig. 5F). These data suggest that the early immunological response is similar between planktonic and biofilm infections.

### Heat-killed bacteria as a model of live infection

To better understand the role of active infection in the immune phenotypes observed in the preceding experiments, wounds were inoculated with preparations of planktonic, heat-killed (HK) *P. aeruginosa* rather than live bacteria and the local immune response was examined (Fig. 6A). Analysis of immune cell infiltrates revealed a significant increase in skin neutrophil populations in response to HK *P. aeruginosa* (Fig. 6B), although the increase was less marked than that seen with live bacteria (Fig. 2B). In addition, the reduction in DC wound infiltrates was no longer significant (Fig. 6C). Separation of the DC wound infiltrates into distinct

subsets did reveal a small but significant decrease in CD103<sup>+</sup> DCs (Fig. 6D) and a trend toward decrease in the other populations. In light of these data, we conclude that treatment with HK *P. aeruginosa* only induces a short-term inflammatory state.

Cytokine mRNA regulation of wounds inoculated with HK PAO1 was also examined and an overall decrease in inflammatory cytokine transcript levels compared with wounds treated with PBS was observed (Fig. 6E). This was in stark contrast with the inflammatory response seen in infections with live bacteria (Fig. 5F). These data suggest that treatment with HK *P. aeruginosa* induces short-lived inflammatory responses, which enter the resolution stage earlier, compared with infections with live bacteria.

## DISCUSSION

We describe a mouse model of chronic *P. aeruginosa* infection that enabled the assessment of wound infection over a 10-day time frame. This model used conventional C57Bl6 mice, did not require immune manipulation or foreign materials, and did not lead to excessive morbidity and mortality. This model therefore has advantages over currently available models of chronic/long-term *P. aeruginosa* infection and may facilitate studies of bacterial pathogenesis, host/pathogen interactions, and antibiotic susceptibility. Because many wounds are infected in the days after the initial injury, we propose that this model is directly relevant to postoperative wound infections in man.

Using this model, we characterized early and late inflammation both within the wound bed as well as within draining LNs and spleen. These assays were performed using flow cytometric analysis of leukocytes harvested from relevant tissues, thereby making possible comprehensive immunophenotyping and quantification.

We found that early infection was marked by local influx of neutrophils and reductions in NK cells and DC subsets, specifically moDCs and CD11b<sup>+</sup> DCs. MoDCs are known to induce TNF and IL-1 $\beta$  secretion and activate Langerhans cells<sup>26</sup> and skin-tropic T cells.<sup>28</sup> CD11b<sup>+</sup> DCs exhibit similar functions and specifically induce Th2-type responses.<sup>29</sup>

At the systemic level, we observed late-stage reductions in IKDCs and NK cells. These cells typically produce high levels of interferon gamma (IFN $\gamma$ ), a cytokine correlated with improved clinical outcomes in CF patients with *P. aeruginosa*.<sup>30</sup> Several studies in acute pneumonia models demonstrated a critical role for NK cell-secreted IFN $\gamma$  in protection against *P. aeruginosa*-induced lethality.<sup>31,32</sup> However, *P. aeruginosa* infection

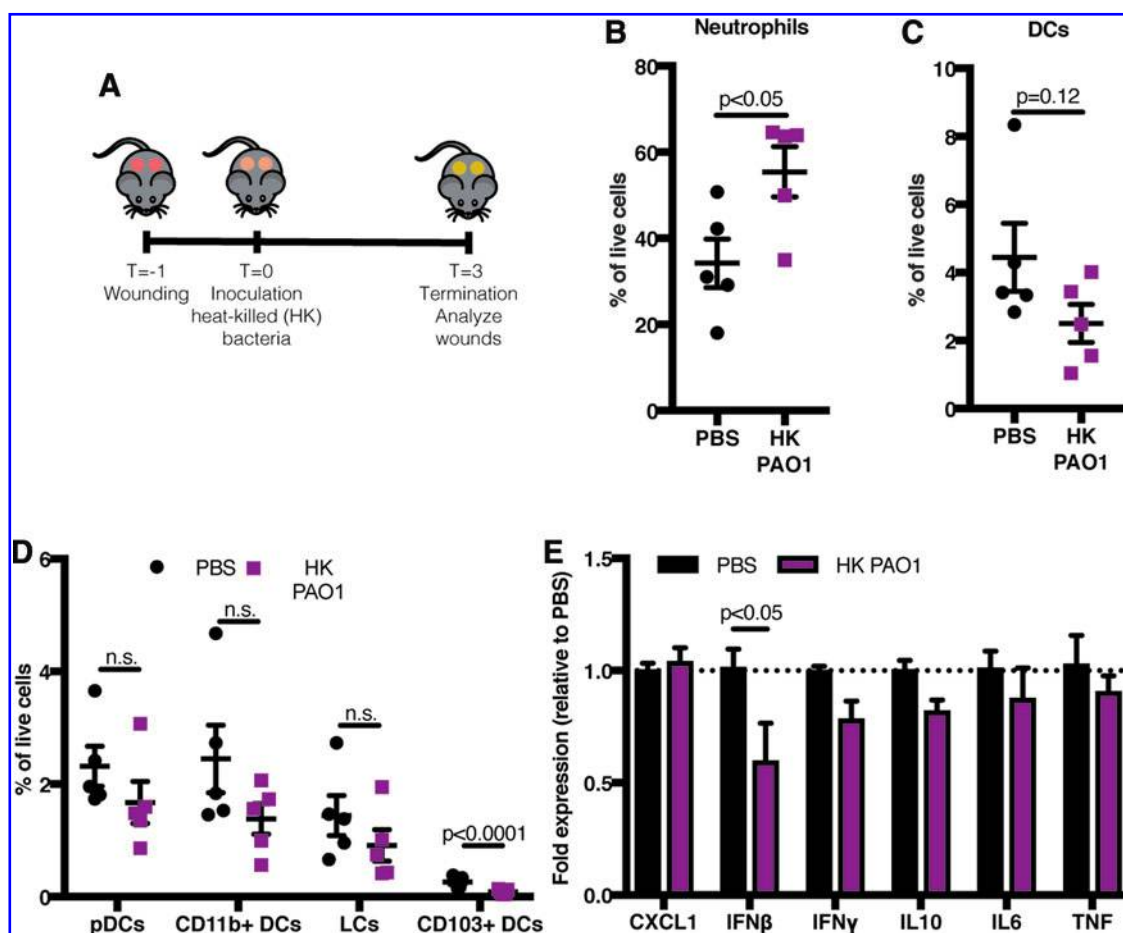


**Figure 6.** HK bacteria as a model of acute wound infection. **(A)** Schematic of the general full-thickness wound inoculation model with HK bacteria. Shown are wound infiltrates for **(B)** neutrophils and **(C)** DCs in the wounds of mice inoculated with HK PAO1 according to the schematic in **(A)**. Statistics are two-tailed Student's *t*-test. **(D)** Wound DC infiltrates from **(C)** divided into distinct DC subsets. Statistics are two-way ANOVA corrected with Sidak multiple comparison. **(B–D)** depict mean with SEM and are representative of  $n \geq 3$  experiments. **(E)** mRNA fold expression (relative to PBS) of several inflammatory cytokines at the wound site after inoculation with HK PAO1 using Pbgd as a household gene.  $n = 5$  wounds/group. Statistics are two-way ANOVA with Dunnett multiple comparison to PBS. Plot depicts mean with SD and is representative of  $n \geq 3$  experiments. HK, heat-killed; LCs, langerhans cells. Color images are available online.

leads to large amounts of NK cell death due to phagocytosis-induced apoptosis.<sup>33</sup> This mechanism is probably at play in our studies, considering we observed a systemic decrease in NK cells and no upregulation of IFN $\gamma$  at the wound bed.

Interestingly, we also observed early and sustained induction of pDCs in the draining LN. A rare immune cell population, pDCs are typically associated with viral infection through their ability to secrete protective type I interferons. However, they have been shown to be critical in the induction of inflammatory responses and the regulation of T cell responses during infection with the intracellular bacterial pathogen *Listeria monocytogenes*,<sup>34</sup> although their depletion did protect from infection-induced mortality. How pDCs are activated during bacterial infection is unknown; this remains a topic for future investigation.

Despite these factors that can impact cells of the adaptive immune response, neither T nor B cells were significantly induced at any time during infection with *P. aeruginosa*. It is possible that our infection model was too short to see truly robust induction of T or B cell populations, or that phenotyping into distinct T cell subsets was necessary to identify nuanced effects.

## INNOVATION

We described the development and validation of a novel delayed inoculation wound infection model of *P. aeruginosa* that offers multiple advantages over existing models. Inoculation of wounds 24 h postsurgery allowed for the adhesion of planktonic bacteria to the scab covering the wound bed, resulting in infection that lasts for at least 7 days

without the use of foreign materials or immunosuppressive mouse phenotypes. The luminescent reporter model outlined in Fig. 1 could be used to answer specific questions related to the induction of protective immune responses, such as timing and localization of immunity.

## ACKNOWLEDGMENTS AND FUNDING SOURCES

The pUT-Tn5-EM7-lux-Km1 luminescent construct vector was a gracious gift from J. Hardy. Special thanks to the laboratory of G. Gurtner for their advice on the wound infection model. Additional thanks to T. Doyle from the Stanford Center for Innovation in *In Vivo* Imaging for his technical expertise. This work was supported by grants R21AI133370, R21AI133240, R01AI12492093, and grants from Stanford SPARK, the Falk Medical Research Trust, and the Cystic Fibrosis Foundation (CFF) to P.L.B. A Gabilan Stanford Graduate Fellowship for Science and Engineering and a Lubert Stryer Bio-X Stanford Interdisciplinary Graduate Fellowship supported J.M.S. A CFF Postdoctoral Fellowship and NIH grant P20GM103546 supported P.R.S.

## AUTHOR DISCLOSURE AND GHOSTWRITING

No competing financial interests exist. The content of this article was expressly written by the authors listed. No ghostwriters were used to write this article.

## ABOUT THE AUTHORS

**Johanna M. Sweere, PhD**, is currently a Consulting Associate at Charles River Associates. She conceived of and developed the wound model that is the subject of this report. **Heather Ishak,**

## KEY FINDINGS

- We report that a delayed inoculation model facilitates chronic wound infection in conventional, healthy C57Bl6 mice. The use of luminescent bacterial strains and flow cytometry greatly facilitate quantitative analysis of infection and immunophenotyping in this model.
- We observed both local and systemic responses to dermal infection in this model.
- Many of the changes in systemic immunity we observed upon infection were in unexpected leukocyte populations, including pDC and NK cells.
- Infections with *P. aeruginosa* biofilms were not more virulent than infections with planktonic *P. aeruginosa* in this model.

**BA, MA**, is currently a laboratory manager at the Palo Alto Veterans Institute for Research. **Vivekananda Sunkari, PhD**, is currently Senior Scientist of R&D and Clinical Data Management at BriaCell Therapeutics. **Michelle S. Bach, BA**, is an undergraduate student at Stanford University. **Robert Manasherob, PhD**, is a research associate at Stanford University. **Koshika Yadava, PhD**, is currently a Postdoctoral Scientist within the MRC Human Immunology Unit at the MRC Weatherall Institute of Molecular Medicine, University of Oxford. **Shannon M. Ruppert, PhD**, is currently a Senior Scientist at Genetech. **Swathi Balaji, PhD**, is an Assistant Professor of Surgery within the Division of Pediatric Surgery at Baylor College of Medicine/Texas Children's Hospital. **Sundeep G. Keswani, MD**, the Director Research at Texas Children's Hospital, of Surgery, Medicine/Texas Children's Hospital, and the Principal Investigator of the LRTR. **Patrick R. Secor, PhD**, is an Assistant Professor of Microbiology at the University of Montana. **Paul L. Bollyky, MD, PhD**, is an Assistant Professor of Infectious Diseases and Microbiology/Immunology at Stanford University. His laboratory studies diabetes and diabetic wound infections.

## REFERENCES

1. Høiby N, Ciofu O, Bjarnsholt T. *Pseudomonas aeruginosa* biofilms in cystic fibrosis. *Future Microbiol* 2010;5:1663–1674.
2. Tredget EE, Shankowsky HA, Rennie R, Burrell RE, Logsetty S. *Pseudomonas* infections in the thermally injured patient. *Burns* 2004;30:3–26.
3. Burgener EB, Sweere JM, Bach MS, Secor PR, Haddock N, Jennings LK, et al. Filamentous bacteriophages are associated with chronic *Pseudomonas* lung infections and antibiotic resistance in cystic fibrosis. *Sci Transl Med* 2019;11:eaau9748.
4. Serra R, Grande R, Butrico L, Rossi A, Settimio UF, Caroleo B, et al. Chronic wound infections: the role of *Pseudomonas aeruginosa* and *Staphylococcus aureus*. *Expert Rev Anti Infect Ther* 2015; 13:605–613.
5. Baum CL, Arpey CJ. Normal cutaneous wound healing: clinical correlation with cellular and molecular events. *Dermatol Surg* 2005;31:674–686; discussion 686.
6. Sadikot RT, Zeng H, Joo M, Everhart MB, Sherrill TP, Li B, et al. Targeted immunomodulation of the NF-kappaB pathway in airway epithelium impacts host defense against *Pseudomonas aeruginosa*. *J Immunol* 2006;176:4923–4930.
7. Mittal R, Sharma S, Chhibber S, Harjai K. Evaluation of tumour necrosis factor-alpha and interleukin-1beta in an experimental pyelonephritis model induced with planktonic and biofilms cells of *Pseudomonas aeruginosa*. *Can J Infect Dis Med Microbiol* 2009;20:e35–e42.
8. Lorè NI, Cigana C, Riva C, De Fino I, Nonis A, Spagnuolo L, et al. IL-17A impairs host tolerance

- during airway chronic infection by *Pseudomonas aeruginosa*. *Sci Rep* 2016;6:25937.
9. Zhao G, Usui ML, Underwood RA, Singh PK, James GA, Stewart PS, et al. Time course study of delayed wound healing in a biofilm-challenged diabetic mouse model. *Wound Repair Regen* 2012;20:342–352.
  10. Watters C, DeLeon K, Trivedi U, Griswold JA, Lyte M, Hampel KJ, et al. *Pseudomonas aeruginosa* biofilms perturb wound resolution and antibiotic tolerance in diabetic mice. *Med Microbiol Immunol* 2012;202:131–141.
  11. van Gennip M, Christensen LD, Alhede M, Qvortrup K, Jensen PO, Hoiby N, et al. Interactions between polymorphonuclear leukocytes and *Pseudomonas aeruginosa* biofilms on silicone implants in vivo. *Infect Immun* 2012;80:2601–2607.
  12. Trøstrup H, Thomsen K, Christophersen LJ, Hougen HP, Bjarnsholt T, Jensen PØ, et al. *Pseudomonas aeruginosa* biofilm aggravates skin inflammatory response in BALB/c mice in a novel chronic wound model. *Wound Repair Regen* 2013;21:292–299.
  13. Secor PR, Sweere JM, Michaels LA, Malkovskiy AV, Lazzareschi D, Katznelson E, et al. Filamentous bacteriophage promote biofilm assembly and function. *Cell Host Microbe* 2015; 18:549–559.
  14. Penner JC, Ferreira JAG, Secor PR, Sweere JM, Birukova M, Joubert L-M, et al. Pf4 bacteriophage produced by *Pseudomonas aeruginosa* inhibits *Aspergillus fumigatus* metabolism via iron sequestration. *Microbiology* 2016;162: 1583–1594.
  15. Sweere JM, Van Bellegehem JD, Ishak H, Bach MS, Popescu M, Sunkari V, et al. Filamentous bacteriophage suppress clearance of bacterial infection. *Science* 2019;363:eaat9691.
  16. Balaji S, Wang X, King A, Le LD, Bhattacharya SS, Moles CM, et al. Interleukin-10-mediated regenerative postnatal tissue repair is dependent on regulation of hyaluronan metabolism via fibroblast-specific STAT3 signaling. *Faseb J* 2017; 31:868–881.
  17. Balaji S, LeSaint M, Bhattacharya SS, Moles C, Dhamija Y, Kidd M, et al. Adenoviral-mediated gene transfer of insulin-like growth factor 1 enhances wound healing and induces angiogenesis. *J Surg Res* 2014;190:367–377.
  18. Kuipers HF, Rieck M, Gurevich I, Nagy N, Butte MJ, Negrin RS, et al. Hyaluronan synthesis is necessary for autoreactive T-cell trafficking, activation, and Th1 polarization. *Proc Natl Acad Sci USA* 2016;113:1339–1344.
  19. Gebe JA, Yadava K, Ruppert SM, Marshall P, Hill P, Falk BA, et al. Modified high molecular weight hyaluronan promotes allergen-specific immune tolerance. *Am J Respir Cell Mol Biol* 2017;56:109–120.
  20. Ruppert SM, Falk BA, Long SA, Bollyky PL. Regulatory T-cells resist cyclosporine-induced cell death via CD44-mediated signaling pathways. *Int J Cell Biol* 2015;2015:614297–614307.
  21. Azzopardi EA, Azzopardi E, Camilleri L, Villapalos J, Boyce DE, Dziewulski P, et al. Gram negative wound infection in hospitalised adult burn patients-systematic review and metanalysis. *PLoS One* 2014;9:e95042.
  22. Wonnemberg B, Jungnickel C, Honecker A, Wolf L, Voss M, Bischoff M, et al. IL-17A attracts inflammatory cells in murine lung infection with *P. aeruginosa*. *Innate Immun* 2016;22:620–625.
  23. Ansell DM, Campbell L, Thomason HA, Brass A, Hardman MJ. A statistical analysis of murine incisional and excisional acute wound models. *Wound Repair Regen* 2014;22:281–287.
  24. Chen JS, Longaker MT, Gurtner GC. Murine models of human wound healing. *Methods Mol Biol* 2013;1037:265–274.
  25. Wilgus TA, Roy S, McDaniel JC. Neutrophils and wound repair: positive actions and negative reactions. *Adv Wound Care* 2013;2:379–388.
  26. Singh TP, Zhang HH, Borek I, Wolf P, Hedrick MN, Singh SP, et al. Monocyte-derived inflammatory Langerhans cells and dermal dendritic cells mediate psoriasis-like inflammation. *Nat Commun* 2016;7:1–18.
  27. Costerton JW, Stewart PS, Greenberg EP. Bacterial biofilms: a common cause of persistent infections. *Science* 1999;284:1318–1322.
  28. Tamoutounour S, Guilliams M, Sanchis FM, Liu H, Terhorst D, Malosse C, et al. Origins and functional specialization of macrophages and of conventional and monocyte-derived dendritic cells in mouse skin. *Immunity* 2013;39:925–938.
  29. Connor LM, Tang S-C, Cognard E, Ochiai S, Hilligan KL, Old SI, et al. Th2 responses are primed by skin dendritic cells with distinct transcriptional profiles. *J Exp Med* 2017;214:125–142.
  30. Moser C, Jensen PO, Kobayashi O, Hougen HP, Song Z, Rygaard J, et al. Improved outcome of chronic *Pseudomonas aeruginosa* lung infection is associated with induction of a Th1-dominated cytokine response. *Clin Exp Immunol* 2002;127: 206–213.
  31. Broquet A, Roquilly A, Jacqueline C, Potel G, Caillon J, Asehnoune K. Depletion of natural killer cells increases mice susceptibility in a *Pseudomonas aeruginosa* pneumonia model. *Crit Care Med* 2014;42:e441–e450.
  32. Wesselkamper SC, Eppert BL, Motz GT, Lau GW, Hassett DJ, Borchers MT. NKG2D is critical for NK cell activation in host defense against *Pseudomonas aeruginosa* respiratory infection. *J Immunol* 2008;181:5481–5489.
  33. Chung JW, Piao Z-H, Yoon SR, Kim MS, Jeong M, Lee SH, et al. *Pseudomonas aeruginosa* eliminates natural killer cells via phagocytosis-induced apoptosis. *PLoS Pathog* 2009;5: e1000561.
  34. Takagi H, Fukaya T, Eizumi K, Sato Y, Sato K, Shibasaki A, et al. Plasmacytoid dendritic cells are crucial for the initiation of inflammation and T cell immunity in vivo. *Immunity* 2011;35:958–971.

#### Abbreviations and Acronyms

|              |                                |
|--------------|--------------------------------|
| cDCs         | = conventional (classical) DCs |
| DCs          | = dendritic cells              |
| HK           | = heat-killed                  |
| IFN $\gamma$ | = interferon gamma             |
| IKDCs        | = interferon killer DCs        |
| LN           | = lymph node                   |
| MoDCs        | = monocyte-derived DCs         |
| NK           | = natural killer               |
| PBS          | = phosphate buffered saline    |
| pDCs         | = plasmacytoid DCs             |
| TNF          | = tumor necrosis factor        |

**This article has been cited by:**

1. Mengjie Wu, Andrey Ethan Rubin, Tianhong Dai, Rene Schloss, Osman Berk Usta, Alexander Golberg, Martin Yarmush. 2021. High-Voltage, Pulsed Electric Fields Eliminate *Pseudomonas aeruginosa* Stable Infection in a Mouse Burn Model. *Advances in Wound Care* **10**:9, 477-489. [[Abstract](#)] [[Full Text](#)] [[PDF](#)] [[PDF Plus](#)] [[Supplementary Material](#)]
2. Chandan K. Sen. 2021. Human Wound and Its Burden: Updated 2020 Compendium of Estimates. *Advances in Wound Care* **10**:5, 281-292. [[Abstract](#)] [[Full Text](#)] [[PDF](#)] [[PDF Plus](#)]
3. Zoya Versey, Waleska Stephanie da Cruz Nizer, Emily Russell, Sandra Zigic, Katrina G. DeZeeuw, Jonah E. Marek, Joerg Overhage, Edana Cassol. 2021. Biofilm-Innate Immune Interface: Contribution to Chronic Wound Formation. *Frontiers in Immunology* **12**. . [[Crossref](#)]
4. Claus Moser, Peter Østrup Jensen, Kim Thomsen, Mette Kolpen, Morten Rybtke, Anne Sofie Laulund, Hannah Trøstrup, Tim Tolker-Nielsen. 2021. Immune Responses to *Pseudomonas aeruginosa* Biofilm Infections. *Frontiers in Immunology* **12**. . [[Crossref](#)]
5. Ruiqi Jia, Kuili Cui, Zhenkui Li, Yuan Gao, Bianfang Zhang, Zhixia Wang, Junwei Cui. 2020. NK cell-derived exosomes improved lung injury in mouse model of *Pseudomonas aeruginosa* lung infection. *The Journal of Physiological Sciences* **70**:1. . [[Crossref](#)]
6. Hannah Trøstrup, Anne Sofie Boe Laulund, Claus Moser. 2020. Insights into Host–Pathogen Interactions in Biofilm-Infected Wounds Reveal Possibilities for New Treatment Strategies. *Antibiotics* **9**:7, 396. [[Crossref](#)]
7. Elizabeth B. Burgener, Patrick R. Secor, Michael C. Tracy, Johanna M. Sweere, Elisabeth M. Bik, Carlos E. Milla, Paul L. Bollyky. 2020. Methods for Extraction and Detection of Pf Bacteriophage DNA from the Sputum of Patients with Cystic Fibrosis. *PHAGE* **1**:2, 100-108. [[Abstract](#)] [[Full Text](#)] [[PDF](#)] [[PDF Plus](#)]
8. Harrison Strang, Aditya Kaul, Umang Parikh, Leighanne Masri, Swetha Saravanan, Hui Li, Qi Miao, Swathi Balaji. Role of cytokines and chemokines in wound healing 197-235. [[Crossref](#)]